Electron-Cloud Instabilities

A. V. Burov*and N. S. Dikansky
Budker INP, 630090, Novosibirsk, Russia

July 5, 1997

Abstract

Photons emitted by a stored beam hit a vacuum chamber surface and produce electrons. These photoelectrons interacts with the beam and can be responsible for the beam transverse instability. The photoelectron instability was suggested by Ohmi to describe phenomena observed at KEK PF [1]. Similar effects were seen at BEPC [2] and CESR [13]. At certain conditions, the electrons can be accelerated by the beam to such a degree that an average secondary emission yield per one primary electron becomes higher than one, the effect first observed at ISR [3]. This phenomenon was payed attention at [4], where analytical estimations were suggested, primarily for PEP-II LER. In fact, the avalanche of secondary electrons is not sensitive to an origin or quantity of initial electrons: the electron density growth rate depends on the secondary emission yield per one absobed electron. This is independent on the density itself until the space-charge limit, being only determined by the beam current, the bunch separation and the vacuum chamber.

Simulations for PEP-II LER [5] showed that the avalanch instability is prevented by TiN coating of that vacuum chamber, the growth rate of the dipole oscillations due to the interaction with primary electrons was numerically found. According to numerical results of [6], the avalanche instability should take place for the LHC, resulting in the space-charge dominated electron cloud.

The paper presented is structured in the following way. First, an analytical model of an electron response on beam transverse oscillations is presented, the transverse impedance and the instability growth rate are found, mainly for a case of factories with rather small bunch separations, $s \simeq 1$ m. Then, the problem of secondary electron density growth (decay) rate is treated analytically and numerically. Finally, estimations for specific case of the LHC are suggested.

1 Steady-State Response

The electron cloud established in a vacuum chamber is a medium which responses on a beam fluctuation and forgets it after a time. Electrons fly out of the chamber surface and

*E-Mail: Burov@inp.nsk.su

live some time inside the volume before they reach the surface again and are absorbed by it. The electron lifetime τ is determined by their average velocity βc and the aperture b:

$$\tau \simeq b/(\beta c).$$

During their lifetime , the electrons are influenced by $M_c \simeq b/(\beta s)$ bunches of the circulating beam, with s as a bunch separation. In factories, the separation is to be rather small, $\simeq 0.6 - 1.2$ m, so electrons with an energy $E_i \simeq 5$ eV have a time to interact with $M_c \simeq 8 - 12$ bunches, providing a possibility for coupled-bunch instabilities. For most dangerous coupled-bunch modes, these $M_c \gg 1$ bunches acts in phase, so, the bunched beam can be treated as a coasting one with the same average current.

Beam oscillations y_+ can be described by an equation of motion, where an electric field induced by the electron cloud E_- is taken into account:

$$\frac{d^2 y_+}{dt^2} + \omega_b^2 y_+ = \frac{eE_-}{\gamma m_+}, \tag{1}$$

with $d/dt = \partial/\partial t + c\partial/\partial z$, ω_b as a betatron frequency, m_+ as a mass of a circulating particle, γ as the relativistic factor. The induced electric field E_- is a linear response on a beam dipole moment, it can be presented in terms of the transverse impedance $Z^\perp$ and the beam current $I_+ = eN_b c/s$:

$$E_- C = iI_+ y_+ Z^\perp,$$

with C as a ring circumference. Assuming $y_+ \propto \exp -i\Omega t + ikz$, the coupled-bunch frequency Ω is found:

$$\begin{aligned} \Omega = & \ \omega_b + ck - i\frac{eI_+ Z^\perp}{2\omega_b C\gamma m_+} \\ \Lambda = & \ \mathrm{Im}\Omega = -\frac{eI_+ \mathrm{Re} Z^\perp}{2\omega_b C\gamma m_+}, \end{aligned} \tag{2}$$

where the impedance $Z^\perp = Z^\perp(\Omega) \approx Z^\perp(\omega_b + ck)$.

In order to find the impedance, the dipole field of the electron cloud E_- can be estimated in terms of its displacement y_- and density n_- assumed to be homogeneous:

$$E_- = 2\pi n_- e y_-, \quad n_- = N_-/(CS),$$

with S as a chamber cross section.

The density n_- results from a steady state solution, while the displacement y_- is found as a dynamic response on the beam dipole oscillations. The electron density is proportional to the total number of particles in the circulating beam $N_+ = N_b C/s$. Assuming , and introducing a compensation factor $\mathcal{P}$, the electron density can be expressed as

$$n_- = \mathcal{P} N_b/(Ss), \quad \mathcal{P} = N_-/N_+. \tag{3}$$

The electron yield per one photon $\eta_{\gamma e}$ is not well known up to now. It is conventional to estimate $\eta_{\gamma e} \simeq 0.1/(1-\mathcal{R})$, where $\mathcal{R}$ is a photon reflectivity: $0.1 \leq \mathcal{R} \leq 0.9$; thus, $0.1 \leq \eta_{\gamma e} \leq 1$.

Taking into account that a photon yield per single particle per revolution $\Delta N_\gamma/N_+ = (5\pi/\sqrt{3})\alpha\gamma$, the compensation factor of the primary electrons is found:

$$\mathcal{P} = \frac{5\pi}{\sqrt{3}}\frac{\tau}{T_0}\alpha\gamma\eta_{e\gamma}, \tag{4}$$

where α is the fine structure constant, T_0 is the revolution period, $\tau/T_0 = M_c/M$, M is the total number of circulating bunches. If the reflectivity is not high, $1-\mathcal{R} \simeq 1$, the compensation writes

$$\mathcal{P} \simeq \alpha\gamma\tau/T_0, \tag{5}$$

The electron space charge results in a run-away of the new-born secondary electrons before the next bunch comes. This limits the compensation factor

$$\mathcal{P} \leq \frac{b\beta_i}{N_b r_e}, \tag{6}$$

$\beta_i = 2E_i/mc^2 = 4.5 \cdot 10^{-3}$.

To find the electron displacement y_-, the following factors have to be taken into account. First, the electrons are converted from the synchrotron photons, which vertical offset follows the beam. Therefore, the emitted electrons have the same initial offset, reduced by the photon reflectivity: $y_+(1-\mathcal{R})$. Second, the electrons are influenced by the electric field of the displaced beam $E_+ \simeq -2e\lambda_+(y_+ - y_-)/b^2$, with λ_+ standing for an average linear density of the beam, $\lambda_+ = N_b/s$. Taking both these factors into account, the electron equations of motion can be presented in the form of a decaying oscillator:

$$\begin{aligned} \frac{dy_-}{dt} &= v_- - \Gamma(y_- - y_+(1-\mathcal{R})) \\ \frac{dv_-}{dt} &= \omega_-^2(y_+ - y_-) - \Gamma v_-, \end{aligned} \tag{7}$$

where $\omega_-^2 \simeq 2\lambda_+ r_e c^2/b^2$ with r_e as the electron classical radius, Γ is an inverse lifetime of the dipole perturbation: $\Gamma = \tau^{-1}$. The electron lifetime $\tau \simeq b/(\beta c)$ is in fact a function of the beam current. If the current is small enough, the electron velocity is determined by its original energy of few eV, $\beta = \beta_i \simeq 5 \cdot 10^{-3}$ and $\tau = \tau_0 \simeq b/(\beta_i c)$. For higher current, the velocity is determined by the beam field itself, which gives $\tau \simeq \omega_-^{-1}$. Thus, the decay rate is estimated $\Gamma = \tau^{-1} \simeq \max\{\omega_-,\ \tau_0^{-1}\}$. Hence, the resonance is broad: $\Gamma \geq \omega_-$.

From here, the response of the electron displacement on the beam one is found:

$$\begin{aligned} y_- &= -iQ(\Omega)y_+, \quad Q(\Omega) = Q_i(\Omega) + Q_d(\Omega) \\ Q_i(\Omega) &= i\,\frac{\Gamma(-i\Omega+\Gamma)}{(-i\Omega+\Gamma)^2+\omega_-^2}(1-\mathcal{R}), \quad Q_d(\Omega) = i\,\frac{\omega_-^2}{(-i\Omega+\Gamma)^2+\omega_-^2}. \end{aligned} \tag{8}$$

The introduced electron response factor $Q(\Omega)$ is a sum of two contributions: $Q = Q_i + Q_d$. First, $Q_i \propto 1-\mathcal{R}$, arises from the initial displacement correlation of the new-born electrons with the corresponding beam particles. This part of the response can be referred to as an instant one. It reaches a maximum at $\Omega \simeq \Gamma$, where $\mathrm{Re}Q_i \simeq \mathrm{Im}Q_i \simeq (1-\mathcal{R})/2$.

The second contribution Q_d is a dynamic one, it describes a driving of the electron oscillations by the beam dipole field. This term also reaches the maximum at $\Omega \simeq \Gamma$, where $\mathrm{Re}Q_d \simeq \mathrm{Im}Q_d \simeq \omega_-^2\tau^2/2$.

For moderate reflectivity, $1-\mathcal{R} \simeq 1$, the instant term estimates result for any current, which gives

$$\max_{\Omega} \mathrm{Re}Q(\Omega) \simeq 1/2 \tag{9}$$

For high reflection, the maximum response is current-dependent, it reaches its limit when the beam field becomes significant: $\omega_-\tau_0 \geq 1$.

Now, the impedance $Z^\perp$ can be expressed in terms of the compensation (Eq. 3) and response (Eq. 8) factors:

$$\frac{Z^\perp(\Omega)}{C} = -\frac{2\pi\mathcal{P}Q(\Omega)}{Sc}. \tag{10}$$

The increment rate Λ (Eq.2) with the impedance (10) can be expressed in terms of the betatron frequency shift on the electron space charge $\delta\omega_b$:

$$\Lambda = \delta\omega_b \mathrm{Re}Q, \quad \delta\omega_b = \frac{N_t r_e c\mathcal{P}}{2\pi\gamma\nu_b b^2}, \tag{11}$$

where $N_t = MN_b$ is a total number of particles in the beam and ν_b is the betatron tune.

If the photon reflectivity is not high, $1-\mathcal{R} \simeq 1$, Eqs.(5, 9) for the compensation and response factors can be used. In this case

$$\Lambda \simeq \frac{(I_+/e)r_e\alpha}{4\pi\nu_b\beta b}. \tag{12}$$

For parameters of the KEK PF, $\nu_b = 3.3$, $b \simeq 3$ cm for $I_+ = 100$ mA it gives for the growth rate $\Lambda \simeq 1500$ s^{-1}. This result is $\simeq 10$ times higher than reported by Ohmi [1] for the same parameters. There are at least two factors distinguishing our model from the approach of Ref.[1].

First, our model takes into account the displacement correlation of the beam and the new-born electrons. If the photon reflectivity is not high, the emitted electrons follow their bunch, which gives an instant contribution in the electron response. When the beam current is not high, $\omega_-\tau \ll 1$, this instant term gives a current-independent impedance. Driving of the electron oscillations by the beam field gives the dynamic contribution in the response, an only one taken into account in Ref.[1]. For low current, this dynamic term results in the impedance proportional to the current itself, giving the increment rate going as the current squared. For the KEK PF parameters, the dynamic response reaches the instant one at $\simeq 300$ mA of the average current; thus, it is $\simeq 3$ times smaller at 100 mA and $\simeq 15$ times smaller at 20 mA, the observed threshold [7] of the instability.

The second factor concerns the wake force prolongation, calculated in the simulations of [1] and estimated in our model. According to the results reported in [1], the prolongation is $\simeq 2$ bunch separations. Instead, we estimate it as the electron lifetime, which is about 5 times higher.

The two factors together give the mentioned order of magnitude difference of our results with Ref.[1].

Some qualitative consequences of the model are discussed below.

- If the current is low, $\omega_-^2\tau^2 < 1$, and the reflection is not high, $1 - \mathcal{R} \simeq 1$, the photoelectron impedance is current-independent. From this point of view, the instability properties for an electron beam have to be the same as for an equal positron beam. This polarity independence was observed at BEPC [8], while it was not observed at KEK PF, perhaps, due to the betatron tune shift of the electron beam on the trapped ions [7, 9]. Then, the suggested model predicts a transformation of the wake force at such a current, when the dynamic response becomes comparable with the instant one, at $\omega_-\tau \simeq 1$. For KEK PF, it gives $\simeq 300$ mA of the average current. This is in agreement with an observed transformation of the betatron sidebands distribution at 240 - 324 mA reported in Ref.[7].

- Above, the vertical beam oscillations were discussed. A difference of the horizontal oscillations is that the instant response of the electrons does not exist for the horizontal direction. Therefore, the horizontal growth rate is suppressed at low current and can be comparable with the vertical one for high current, when $\omega_-\tau \simeq 1$.

- The magnetic field was assumed to be absent in the region of interaction between the beam and the electron cloud. However, the photoelectrons born inside bending parts by scattered photons interact with the beam as well, with the response factor $\simeq \mathcal{R}Q_d$. For small reflectivity $\mathcal{R} \ll 1$, their influence is suppressed. A fraction of 'productive' photons, reaching the aperture outside the bending parts, depends on the closed orbit geometry and may strongly vary with the beam energy.

- The instability growth rate is suppressed when the head-tail phase $\phi_\xi = \xi\omega_b\sigma_b/(c\eta)$ is high enough, $\phi_\xi > 1$ [10]. Here ξ is the chromaticity, σ_b is the bunch length, η is the momentum compaction. The instability damping by the chromaticity increase was observed at BEPC [8] for such parameters that $\phi_\xi \simeq 1$.

2 Secondary Electrons Avalanche

2.1 Estimations

In this section, the established electron density is treated in more details. At the beginning, certain estimates are suggested, and then simulations are presented and discussed.

Electrons arises at the chamber surface with initial energy $E_i = 5 - 10$ eV. Then, they are accelerated and decelerated by the beam, reach again the surface and produce secondary electrons instead of themselves, which again interact with the beam, and the process goes on. In the result, the electron density decays or grows, in the dependence of the secondary emission. In the last case, the process would be stopped due to the space charge of the electrons. A secondary emission yield per an incident electron is determined by its energy E and the angle of incidence θ with respect to the surface normal. Following [11] and [6], the analytical expression for the yield can be taken as

$$\eta_{ee}(E,\theta) = 1.1\hat{\eta}_{ee}E_r^{-0.35}\left(1-\exp\left(-2.3E_r^{1.35}\right)\right)/\cos\theta, \tag{13}$$

with the relative energy $E_r = E/E_m$, $E_m = 250 - 400$ eV. This function has a maximum at $E_r = 1$, where $\eta_{ee} = \hat{\eta}_{ee}/\cos\theta$. The maximum yield parameter $\hat{\eta}_{ee}$ varies from 1.8 (Cu) to 1.1 (NiT). Energies and angles of the hitting electrons are determined by the beam parameters and by geometry of the vacuum chamber. In a chamber with round cross-section, the angles are small, $\cos\theta \cong 1$, while for an asymmetrical cross-section the angle factor is emphasized. Hence, round chambers are more preferable from this point of view and could be used to damp the avalanche instability.

When near the chamber, electrons gain the velocity kick from a single bunch $\delta\beta \cong 2Nr_e/b$. If the bunch separation s is high enough, $s > 2b/\delta\beta$, or $Nr_e s/b^2 > 1$, emitted electrons interact with an only one bunch. A sufficient condition of the stability (decay of the secondary electron density) for a round chamber in this case, according to (13), is $\delta\beta/\delta\beta_c < (\hat{\eta}_{ee})^{-1/2}$ or $\delta\beta/\delta\beta_c > (\hat{\eta}_{ee})^{3/2}$ where $\delta\beta_c = \sqrt{0.8E_m/mc^2} = 0.025\sqrt{E_m/400eV}$. This condition of separated bunches is not satisfied for typical factory parameters: assuming, for instance, $N = 5\cdot 10^{10}$, $b = 3$ cm, it requires $s > 7$ m, while $s = 1.2$ m for PEP-II and $s = 0.6$ m for KEKB projects. At these conditions, the electrons have enough time to interact with many bunches. In the result, the electron energy gain is determined by the strongest kick, occurred at a minimal for a given particle impact parameter r, with the velocity kick $\delta\beta \cong 2Nr_e/r$. When the next bunch comes, it meets the electron at the distance $\cong s\delta\beta - r$, the electron will not run away if only $r < s\delta\beta/2$. If the beam is dense enough, $s \ll b^2/Nr_e$, it looks reasonable to assume electrons crossing the beam area at a random phase of the bunch motion. It follows an estimate for the impact parameter of an accelerated electron: $r \cong s\delta\beta/4$; this gives $\delta\beta = \sqrt{8Nr_e/s}$, comparable with the result at the coasting beam approximation with $\beta = \sqrt{2Nr_e\ln(b/r)/s}$. If this velocity lies in the 'productive' interval, $\delta\beta \cong (1-3)\delta\beta_c$, the avalanche instability have to be expected.

The above estimates give an expression for the parameter of the problem, $J = 8Nr_e/(s\beta_c^2)$ or

$$J = 10\frac{Nr_e}{s}\frac{mc^2}{E_m}. \tag{14}$$

According to the above heuristic ideas, the secondary electron avalanche instability is expected approximately when

$$2/\hat{\eta}_{ee} \le J \le 2\hat{\eta}_{ee}^3.$$

2.2 Simulations for Straight Sections

To have an exact solution for the problem of the secondary electron density decay (growth) rate, the simulation code was prepared and the simulations were run. Vacuum chamber was assumed to be elliptical, $b_y < b_x$. Image charges were taken into account: the electrostatic problem can be resolved analytically in an elliptic coordinates u, v :

$$x = a\cosh u\ \cos v, \quad y = a\sinh u\ \sin v \tag{15}$$

$$a = \sqrt{b_x^2 - b_y^2},\ 0 \le u \le u_0,\ 0 \le v \le 2\pi,$$

with $u = u_0$ corresponding to the chamber surface, $\cosh u_0 = b_x/a$. An electrostatic potential of a beam with a linear density λ is expressed as a fairly fast converging expansion:

$$\Phi(x, y) = -\lambda \left\{ \ln \frac{a}{r} - \sum_{n=1}^{\infty} C_n \cosh(2nu) \cos(2nv) / \cosh(2nu_0) \right\} \tag{16}$$

$$C_n = \frac{2}{\pi} \int_0^{\pi} \ln \frac{a}{r} \cos(2nv)\ dv$$

Initially, electrons are equidistantly placed at the surface with $2D$ energy $E_i = 5 \pm 5$ eV, velocity directions are distributed as a $\cos\theta$ with respect to the surface normal, and a unit weight is assumed for every particle. Then they start and are periodically kicked by the bunches, the kicks are calculated from (16). When an electron reaches the surface, it is reemitted with the described distribution, and its weight changes on a factor of η (13). Therefore, the number of simulated particles conserves, while their total weight W changes. Finally, the electron density decrement rate τ^{-1} was calculated by means of the initial and final weights:

$$\tau^{-1} = -\ln(W_f/W_i)/T = W_i / \int_0^T W(t) dt$$

where T is the time interval; a convergence of the result with the time T were controlled. The decrement is presented at Figs. 1,2,3,4 as a function of the beam intensity J, for yield parameters $1.1 \le \hat{\eta}_{ee} \le 1.8$, round and elliptic chambers and for two bunch separations, 120 and 60 cm. Negative rate means the instability. If it is positive, the steady state electron density may be found as $N_{se} = \dot{N}_{se}\ \tau$, where $\dot{N}_{se}$ is a production rate. The numerical results bring to certain conclusions.

- The density rate significantly varies with the intensity parameter. It is positive in any case, when $\hat{\eta}_{ee} \le 1.2$, which can be considered as a sufficient safe condition. Otherwise, the instability regions at the intensity interval $1.5 \le J \le 25$ take place. When the current is low or high enough, $J \le 1.5$, or $J \ge 25$, the density decays for any $\hat{\eta}_{ee}$ within the declared interval.

- The smaller is the separation, the better. This tendency is obvious: for a coasting beam, the energy of the electrons conserves, and the source for the secondary yield disappears.

- When the bunches are more separated ($s = 120$ cm), the benefit of the round chamber form is more pronounced. It could be caused by the fact that inclined trajectories are longer and the energy gain is decreased for them for less separated bunches due to averaging factor. For the round chamber, the safe condition is $\hat{\eta}_{ee} \le 1.5$.

- For the round chamber, the rate dependences on the intensity have pronounced oscillations. This is caused by variations of the average impact parameters, which are smoothed for the elliptical chamber. In the result, the average energy of electrons on the surface impact have oscillational factor, which is shown on Figs. 5,6.

2.3 Simulations for Bending Sections

The simulations were carried out for bending sections as well. Electrons were considered as magnetized in this case; thus, the horizontal coordinate were fixed. The density decrement was calculated as a function of the horizontal coordinate of the multiplicating particles, and then the minimum over the horizontal position was treated as the decrement rate for given beam and aperture parameters.

The results for the elliptical and round chambers with the separations 120 cm and 60 cm are presented in Figs.7,8,9,10. Several comments follow.

- The electron density can be unstable at the intensity interval $1 \leq J \leq 25$, for bendings as well as for straight sections.
- Angle factor of the secondary emission (13) is emphasized here, which causes the decrease of the decrement rates, in the comparison with the straight section.
- There is no reason for the round chamber benefit, it looks even worse than elliptical one.
- The separations are important, as well as for the straight sections.
- When the bunches are more separated (120 cm), the avalanche instability takes place at certain intensity interval even for lowest yield constant, $\hat{\eta}_{ee} = 1.1$.

3 Electron-Cloud Dynamics for LHC

A simulation study of the electron-cloud instabilities in the LHC was recently carried out by F. Zimmermann [6]. Here, analytical estimations concerning the problem are suggested.

Specific features of the LHC are:

energy $E = 7$ TeV, particles / bunch $N_b = 10^{11}$;

bunch separation $s = 7.5$ m, chamber half-axis (2.3, 1.8) cm;

tunes $\nu_{x,y} = 63.3$;

high weight of the bendings, about 80% of the circumference.

Due to the relatively high separation, emitted electrons have to be slow enough to feel at least one bunch:$\beta < \beta_s \cong 2b_y/s$, which corresponds to energy $E < E_s = mc^2\beta_s^2/2 \cong 5$ eV, somewhat about the average emission energy E_i. The density decrement rate as a function of the intensity parameter (14) for the LHC is shown on Fig.11. According to these results, the e-cloud decays within the considered intervals of the parameters, which is a disagreement with the simulations of Ref.[6], where the avalanche instability is reported to be observed even for the TiN yield constant $\hat{\eta}_{ee} = 1.1$. According to Fig.11, the density decay rate is very close to zero for the Cu case ($\hat{\eta}_{ee} = 1.8$) just at the nominal current with $N_b = 10^{11}$ corresponding to $J = 0.5$; however, for the TiN case the decay is quite fast, $\tau = 2.5s/c$. When this rate is known, the steady-state level of the electron density is determined by Eq.(4). In the magnetic field, this result have to be multiplied on the photon reflectivity $\mathcal{R}$. It gives for the relative electron linear density $\mathcal{P} = N_-/N_+$ with $N_+ = N_b/s$:

$$\mathcal{P} = \frac{5\pi}{\sqrt{3}} \mathcal{R} \eta_{\gamma e} \alpha \gamma \tau / T_0 \tag{17}$$

According to Ref.[12], the photoelectron yield for the LHC parameters $\eta_{\gamma e} \simeq 0.02$; this value is reported in [6] as significantly higher: $\eta_{\gamma e} \simeq 0.1$. The reflectivity is also fairly uncertain: $0.2 < \mathcal{R} < 1$. Thus, the factor $\mathcal{R}\eta_{\gamma e}$ have different orders of magnitude for its upper and lower limits: $0.004 < \mathcal{R}\eta_{\gamma e} < 0.1$. For the TiN coated walls ($\hat{\eta}_{ee} = 1.1$) the electron density life time, according to Fig.11, $\tau = 2.5s/c$. At the worst case with $\mathcal{R}\eta_{\gamma e} = 0.1$ it results in $\mathcal{P} = 0.03$, which is an order of magnitude smaller than the electron space-charge limit (6).

In the magnetic field, the electron density is a function of the horizontal coordinate. A horizontal offset of the beam changes local electron energy gains, which causes a displacement of the electron distribution. When the frequency of the beam horizontal oscillations $\omega = \omega_0 (\nu - n)$ is smaller than the electron distribution relaxation rate τ^{-1}, the electron density offset x_- follows the beam:

$$x_- = \frac{x_+}{1 - i\omega\tau}; \quad \mathrm{Im}\frac{x_-}{x_+} \leq 1/2.$$

Substituting these values in the equation of motion

$$\ddot{x}_+ + \omega_b^2 x_+ = eE_-/(\gamma M)$$

with $eE_- = 2\lambda_- e^2 x_-/b^2$, $\lambda_- = \mathcal{P}N_b/s$, the instability rate of the horizontal betatron oscillations writes:

$$\Lambda_x = \frac{\mathcal{P}N_b r_p c\bar{R}}{2\gamma\nu_b s b^2}, \tag{18}$$

where $\bar{R}$ is an average radius of the ring. For $\mathcal{P} = 0.03$, it gives the growth rate $\Lambda_x^{-1} = 0.5$ s. The same kind of estimations brings to the vertical increment rate:

$$\Lambda_y = \Lambda_x \beta_i/\beta, \quad \beta = 2N_b r_e/b \gg \beta_i, \tag{19}$$

resulting in $\Lambda_y^{-1} = 3$ s. These numbers are very sensitive to the wall material. For Cu ($\hat{\eta}_{ee} = 1.8$) the electron density life time is more than order of magnitude higher. In this case, the steady-state electron density could reach the space-charge dominated level (6), which estimates in $\mathcal{P} \cong 0.5$. If so, the estimations above (18,19) give the values closed to the numerical results of Ref.[6]: $\Lambda_x^{-1} = 30$ ms, $\Lambda_y^{-1} = 180$ ms. However, the high uncertainty in the photoelectron yield and the photon reflectivity does not permit to give definite numbers.

4 Acknowledgments

The authors are thankful to O. B. Malyshev for discussions concerning photoelectron emission and to S. A. Heifets for information.

References

[1] K. Ohmi, Phys. Rev. Lett., **75**, No 8, p. 1526 (1995).

[2] Z. Y. Guo et. al., PAC-97.

[3] O. Gröbner, Proc of X Int. Conf. on High Energy Accel., Protvino, 1977.

[4] S. A. Heifets, in CEIBA95, p.295.

[5] M. Furman and G. Lambertson, in PEP-II Design Reports, 1995, 1997.

[6] F. Zimmerman, LHC Report 95, 1997

[7] M. Izawa, Y. Sato and T. Toyomasu, Phys. Rev. Lett., **74**, No 25, p. 5044 (1995).

[8] H. Fukuma, *private communication*, 03 Jan 1997.

[9] Photon Factory Activity Report No. 7, 1989, p. R-8.

[10] A. W. Chao, *Physics of Collective Beam Instabilities in High Energy Accelerators*, J. Wiley & Sons, Inc., 1993.

[11] H. Seiler, J. Appl. Phys. **54**, 11, 1983.

[12] O. Gröbner, PAC, 1997.

[13] Holmquist

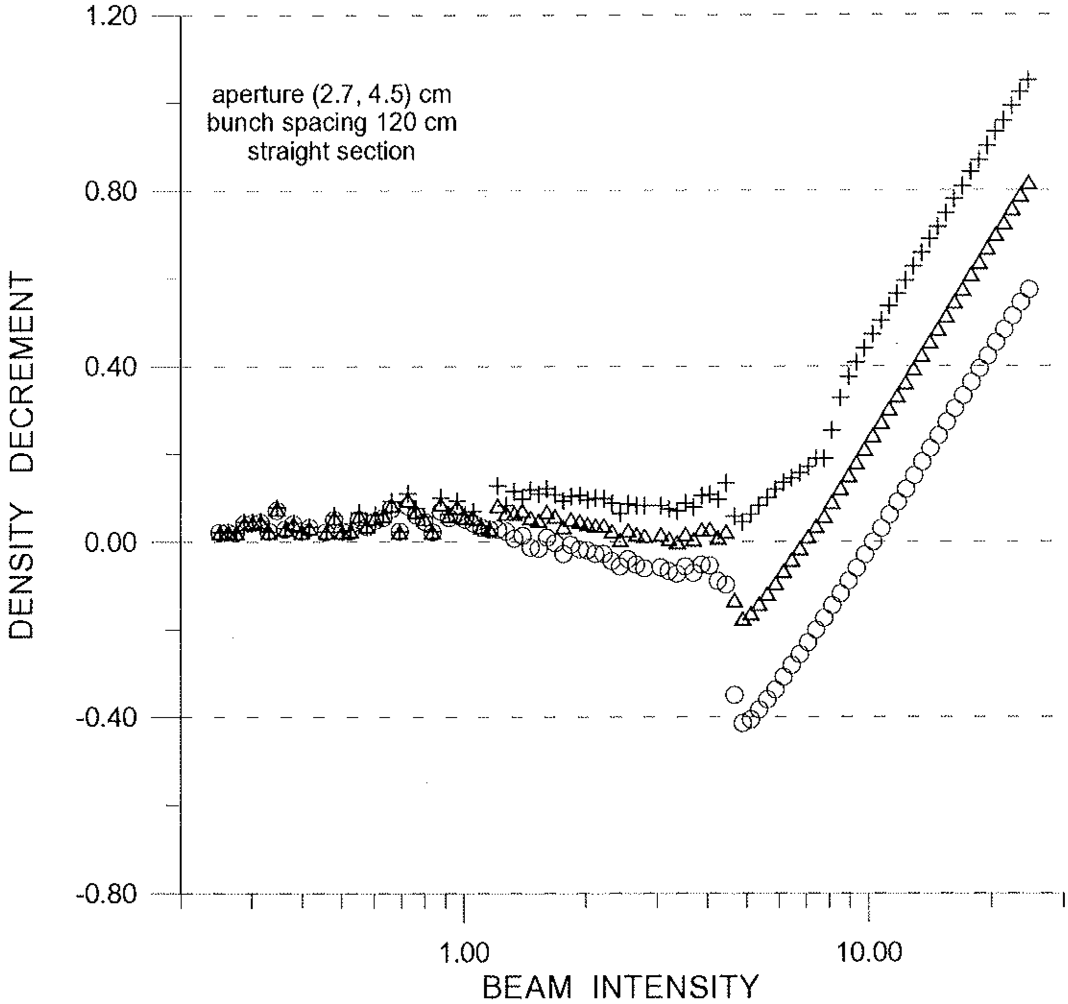

Figure 1: Electron density decay rate for various secondary emission yield constants $\hat{\eta}$: 1.1, 1.4 and 1.8, labeled by $+$, $\triangle$ and $\circ$ correspondingly. The vacuum chamber and beam separations are taken as PEP-II.

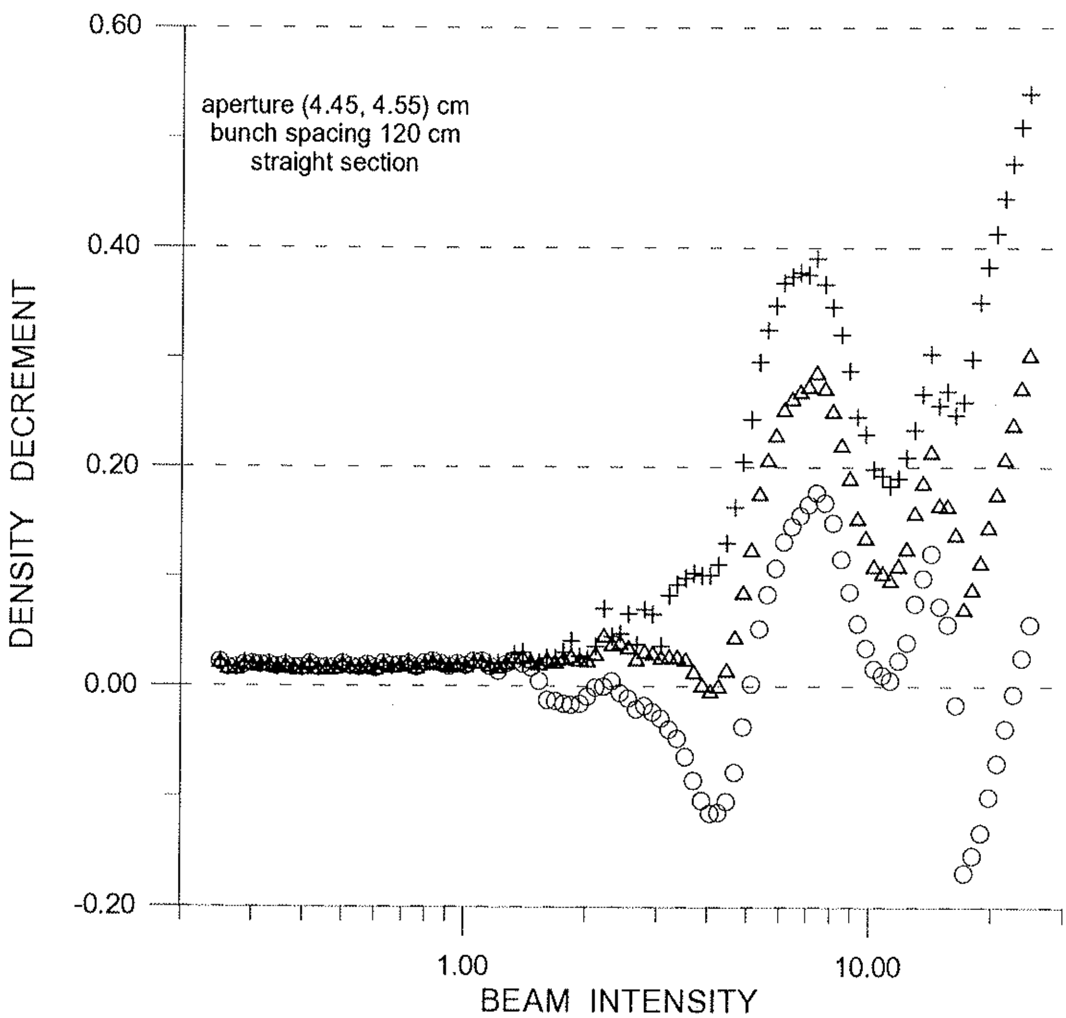

Figure 2: The same as previous figure, but the chamber is round.

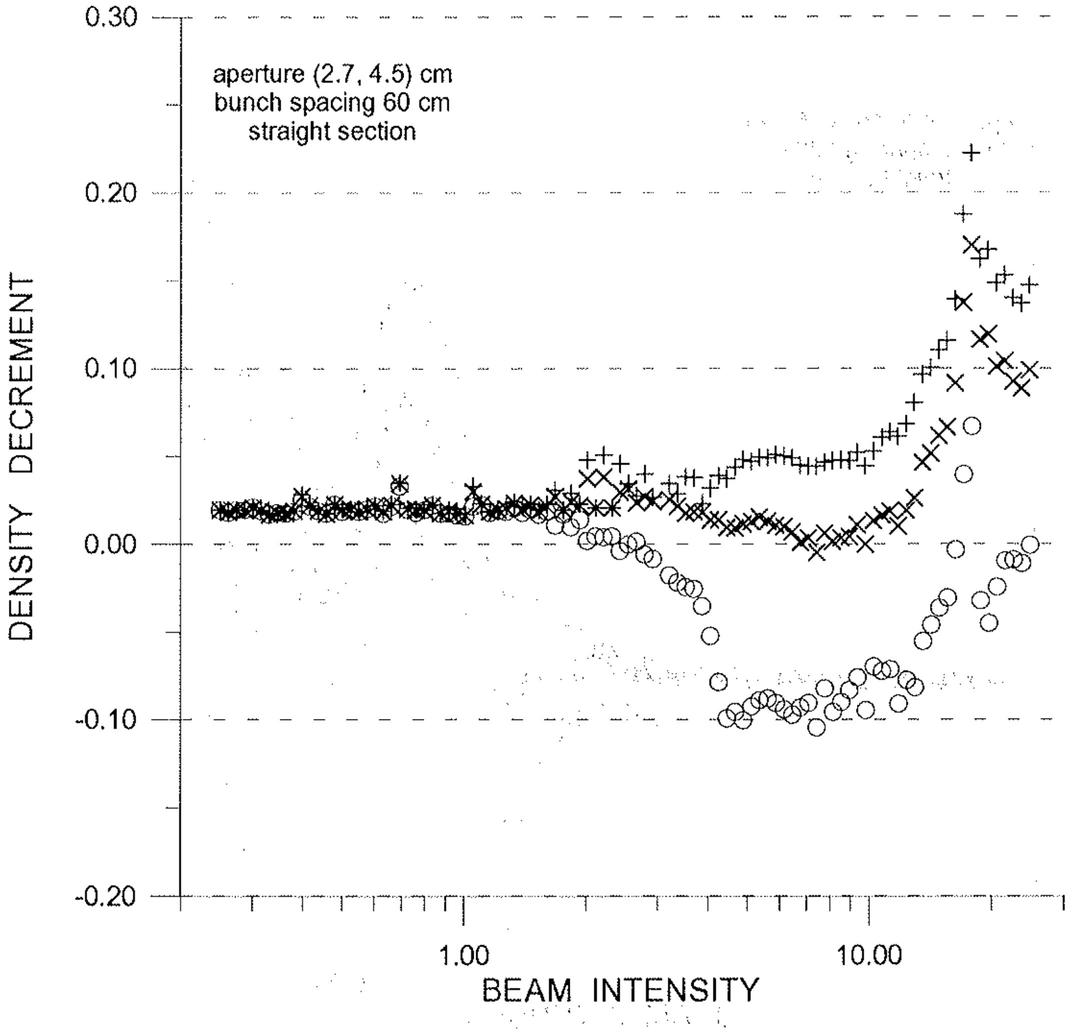

Figure 3: The chamber and spacings are for KEKB project. The yield constants $\hat{\eta}$ are 1.1, 1.3 and 1.8 marked by $+$, $\times$ and $\circ$.

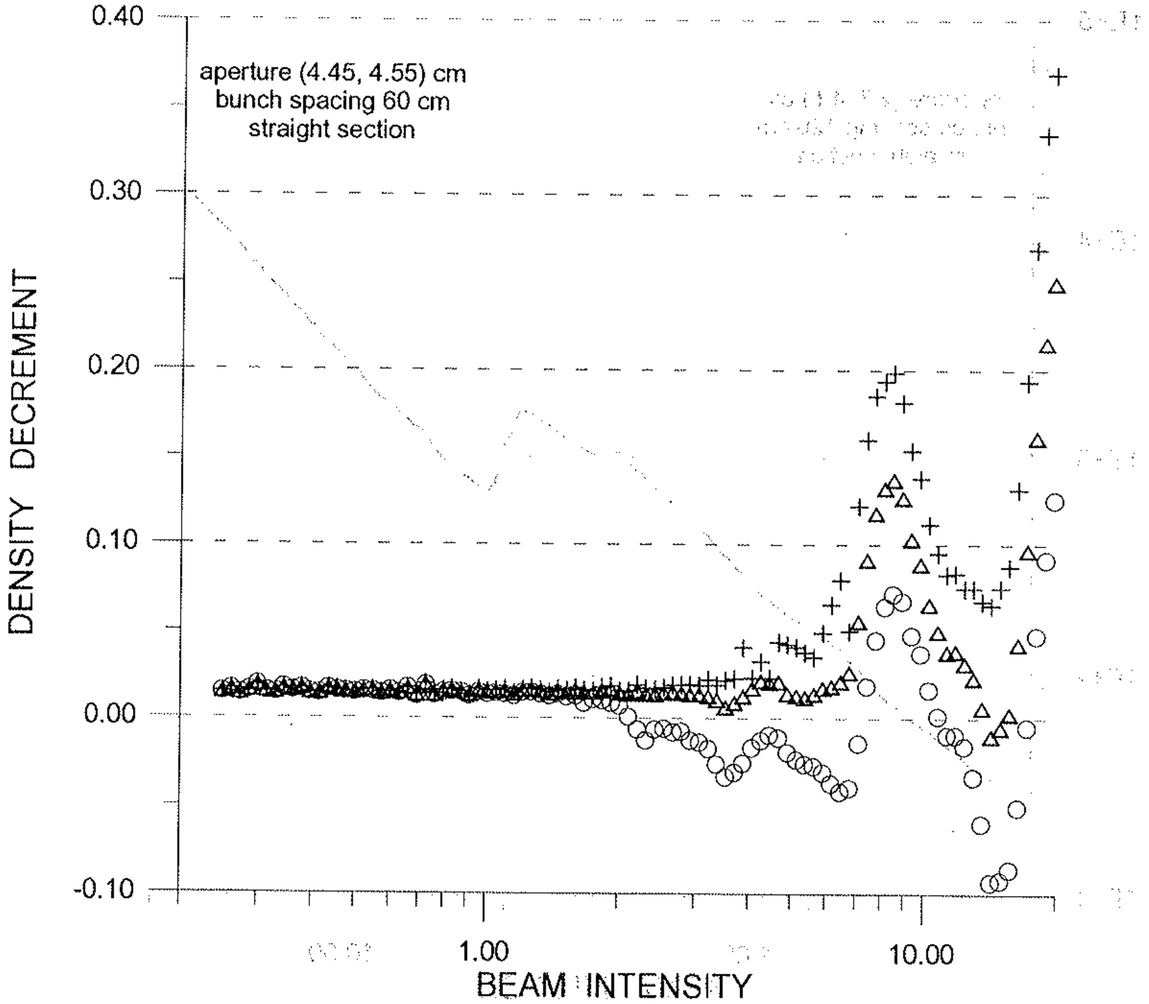

Figure 4: Same spacings as previous, but the chamber is round. The yield constants $\hat{\eta}$ are 1.1, 1.4 and 1.8 marked by $+$, $\triangle$ and o.

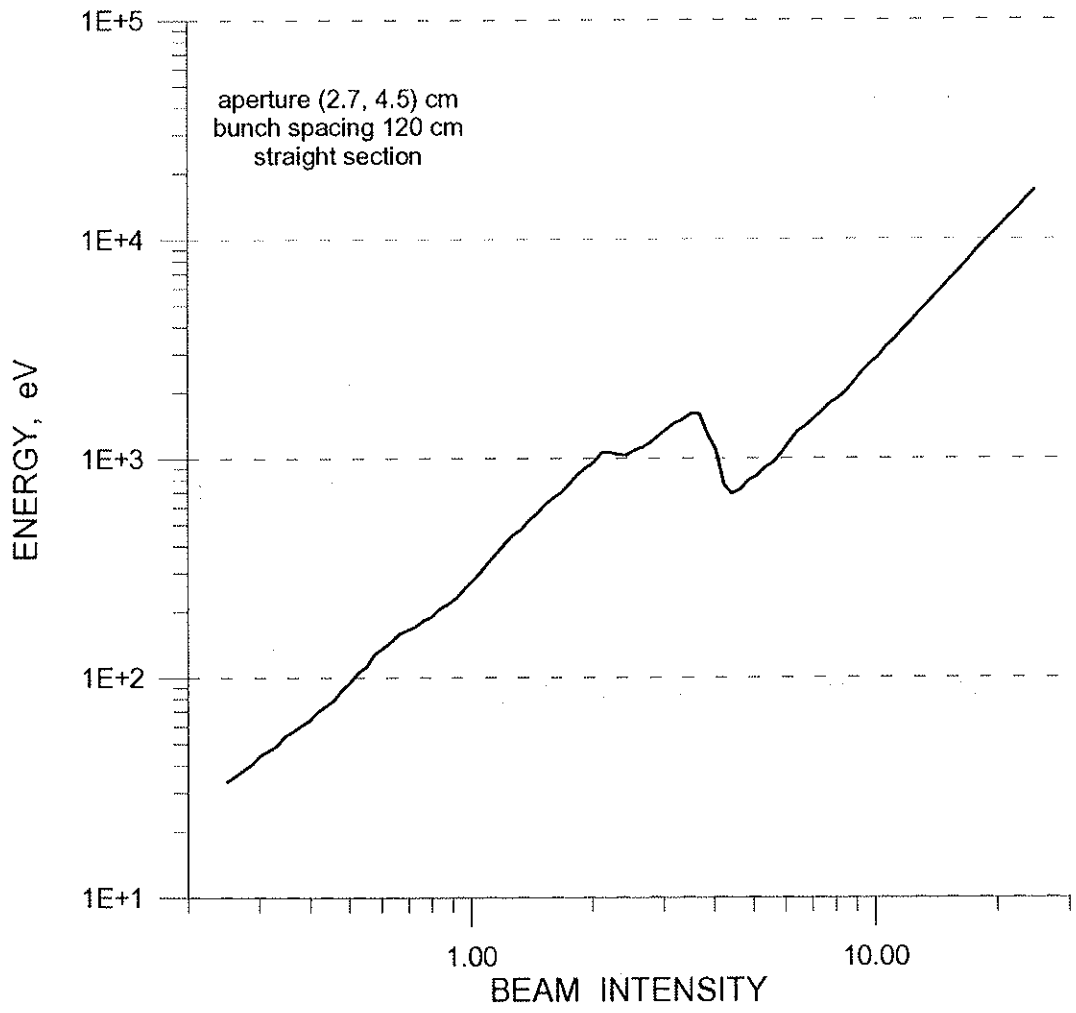

Figure 5: Average electron energy as a function of beam current for the PEP-II parameters.

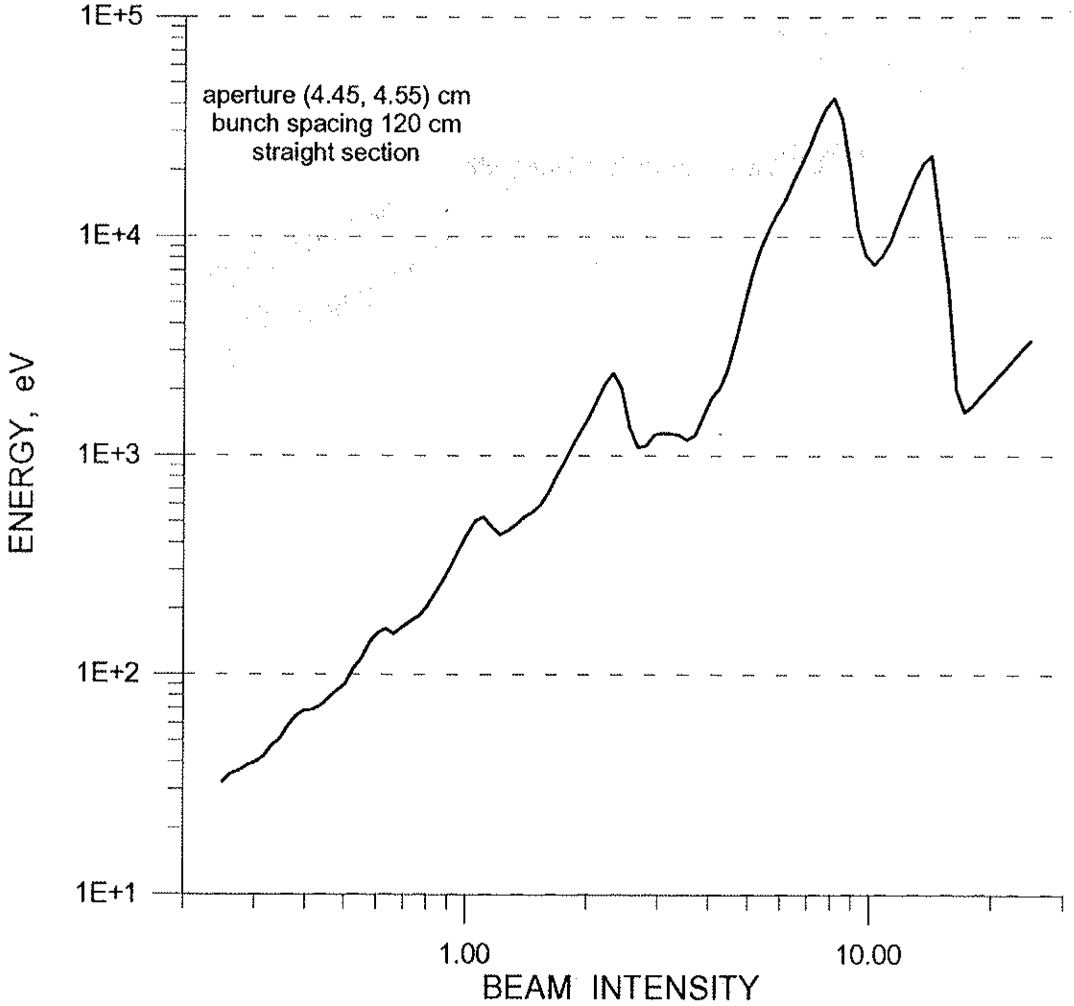

Figure 6: The same, but for the round chamber.

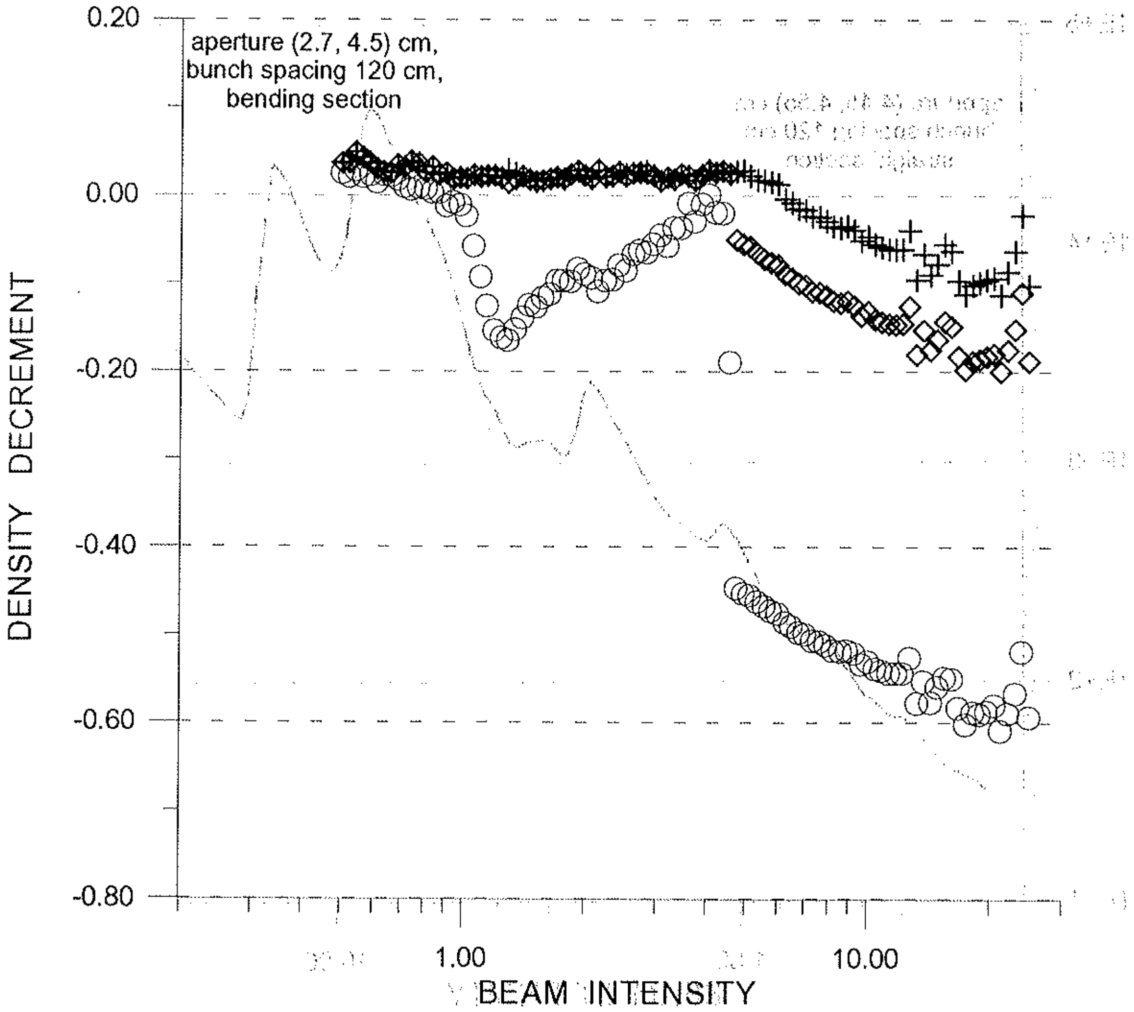
0.20
0.00
-0.20
-0.40
-0.60
-0.80
DENSITY DECREMENT
aperture (2.7, 4.5) cm,
bunch spacing 120 cm,
bending section
1.00
10.00
BEAM INTENSITY

Figure 7:

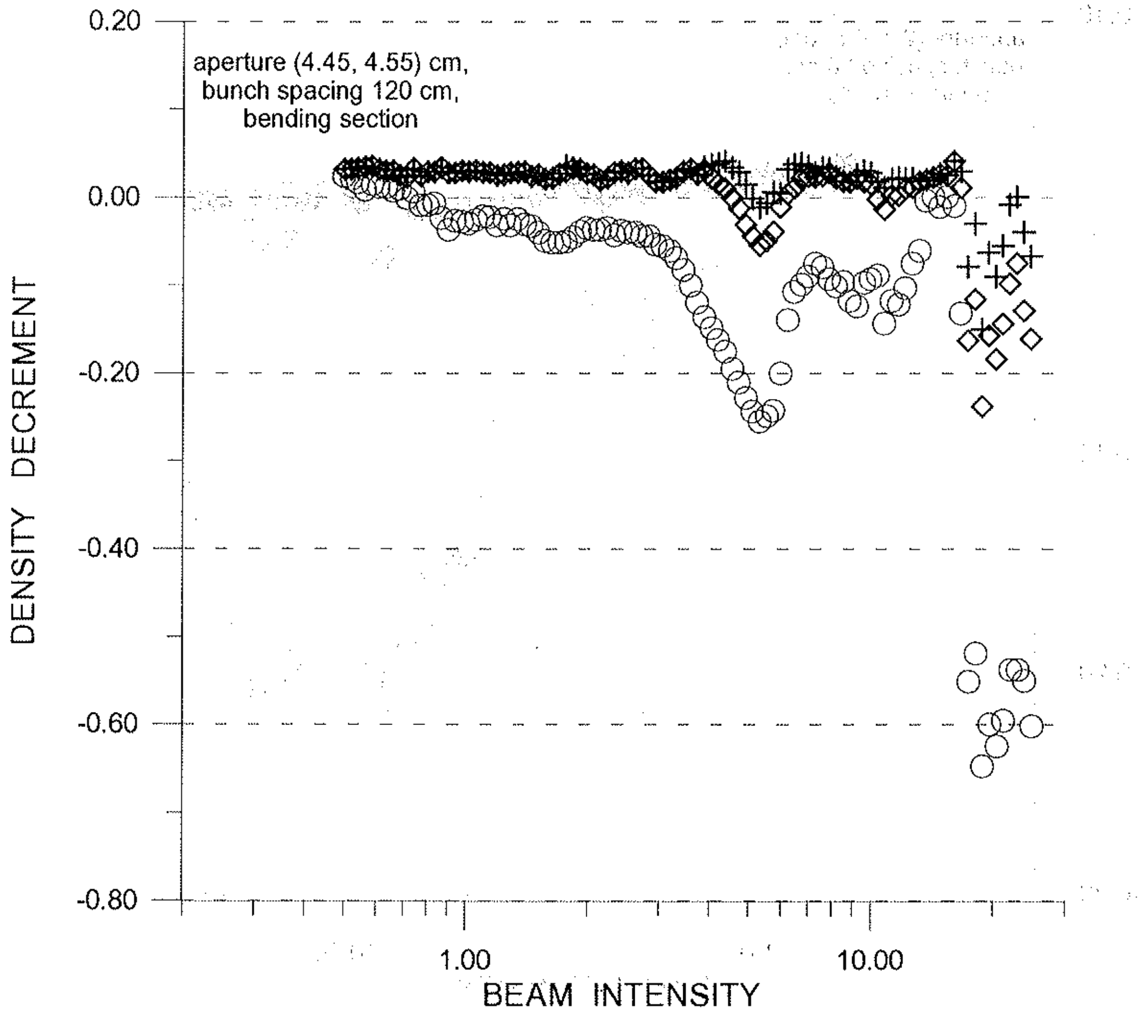

aperture (4.45, 4.55) cm,
bunch spacing 120 cm,
bending section
0.20
0.00
-0.20
-0.40
-0.60
-0.80
DENSITY DECREMENT
1.00
10.00
BEAM INTENSITY

Figure 8:

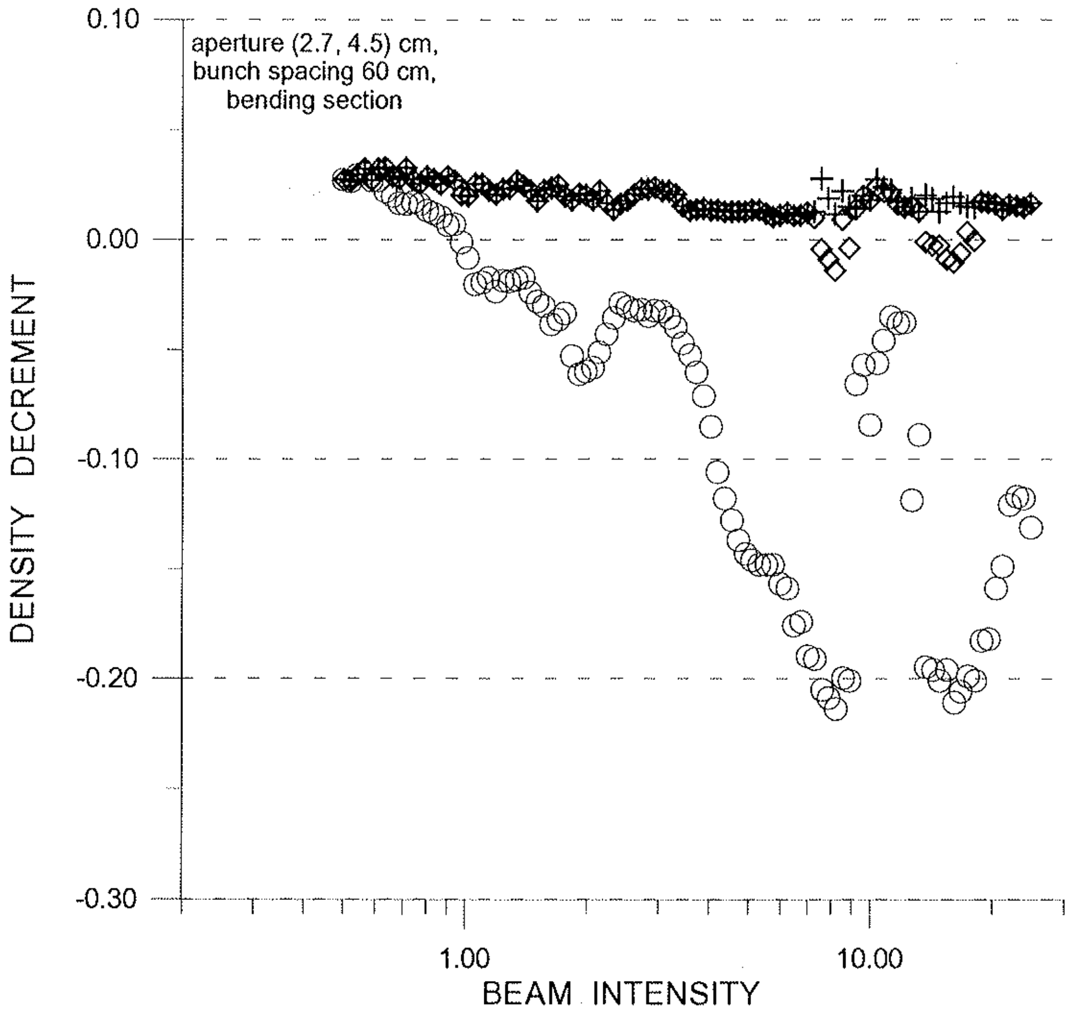

aperture (2.7, 4.5) cm,
bunch spacing 60 cm,
bending section
0.10
0.00
-0.10
-0.20
-0.30
DENSITY DECREMENT
1.00
10.00
BEAM INTENSITY

Figure 9:

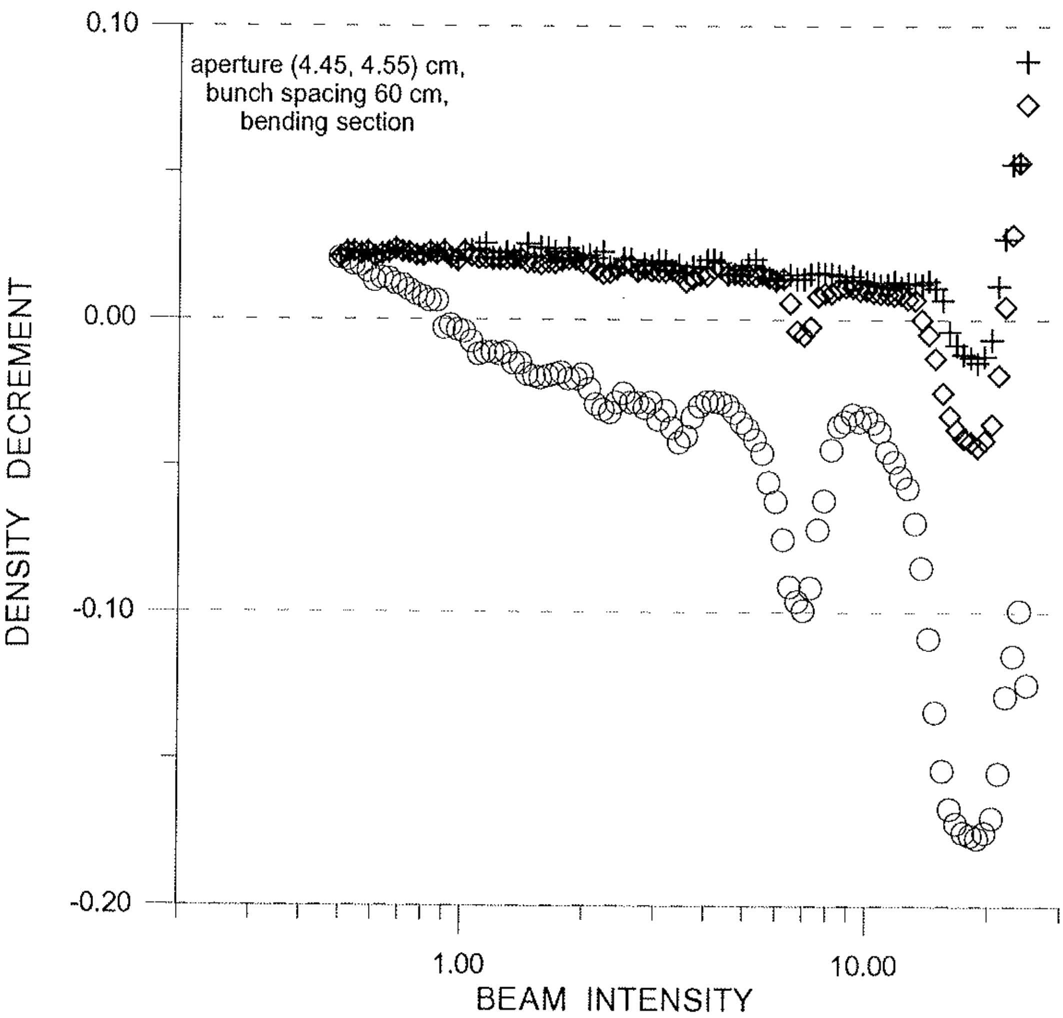
0.10
0.00
-0.10
-0.20
aperture (4.45, 4.55) cm,
bunch spacing 60 cm,
bending section
DENSITY DECREMENT
1.00
10.00
BEAM INTENSITY

Figure 10:

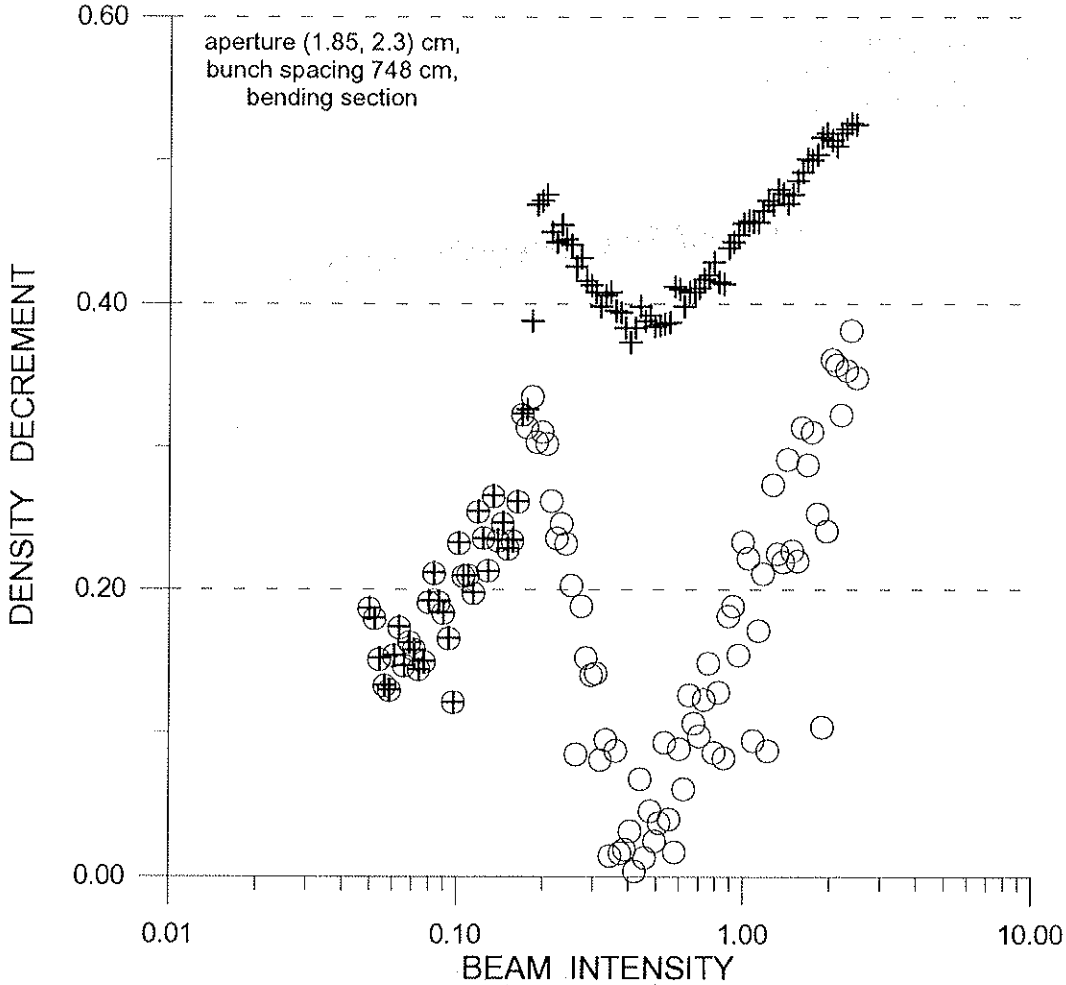
aperture (1.85, 2.3) cm,
bunch spacing 748 cm,
bending section
0.60
0.40
0.20
0.00
DENSITY DECREMENT
0.01
0.10
1.00
10.00
BEAM INTENSITY

Figure 11: